



**HAL**  
open science

## Shape memory through contact : introduction of magnetofriction – shape memory polymers (MF-SMPs)

Svenja Hermann, Pauline Butaud, Gael Chevallier, Laurent Hirsinger, Morvan Ouisse

### ► To cite this version:

Svenja Hermann, Pauline Butaud, Gael Chevallier, Laurent Hirsinger, Morvan Ouisse. Shape memory through contact : introduction of magnetofriction – shape memory polymers (MF-SMPs). SPIE Smart Structures + Nondestructive Evaluation 2022, Mar 2022, Orlando, United States. hal-03813034

**HAL Id: hal-03813034**

**<https://hal.science/hal-03813034>**

Submitted on 13 Oct 2022

**HAL** is a multi-disciplinary open access archive for the deposit and dissemination of scientific research documents, whether they are published or not. The documents may come from teaching and research institutions in France or abroad, or from public or private research centers.

L'archive ouverte pluridisciplinaire **HAL**, est destinée au dépôt et à la diffusion de documents scientifiques de niveau recherche, publiés ou non, émanant des établissements d'enseignement et de recherche français ou étrangers, des laboratoires publics ou privés.

# Shape Memory through Contact : Introduction of MagnetoFriction – Shape Memory Polymers (MF-SMPs)

Svenja Hermann<sup>a</sup>, Pauline Butaud<sup>a</sup>, Gael Chevallier<sup>a</sup>, Laurent Hirsinger<sup>b</sup>, and Morvan Ouisse<sup>a</sup>

FEMTO-ST Institute, CNRS/ENSMM/UTBM/UBFC, F-25000 Besançon, France

<sup>a</sup>Applied Mechanics Department

<sup>b</sup>Micro Nano Sciences and Systems Department

## ABSTRACT

Materials that have a shape memory are capable to switch between different stable states when external stimuli are applied. This work introduces a new, multi-physical concept for shape memory in assembled composite structures. The concept is called magnetofriction and is based on magnetism, elasticity, contact and friction. In assemblies of permanently magnetized MagnetoActive Elastomers (MAE), the contact pressure is established by magnetic attraction forces. When the assembly is deformed, the contact surfaces slide over each other and the deformed shape is locked by the friction in the interface. A loosening of the contact causes the friction forces to vanish and each part of the assembly recovers its initial state due to the elastic forces in the materials. The contact is restored after the shape recovery. A test assembly, called MagnetoFriction – Shape Memory Polymer (MF-SMP), is used to validate the concept experimentally. It consists of two stacked, permanently magnetized MAE beams. The assembled structure is subjected to a three-point bending test and retains a permanent deformation after the tests. The force displacement response of the MF-SMP reveals that the deformed configuration is stabilized after a first loading cycle. A digital image correlation reveals sliding in the contact interface of the assembly during the first loading. The adhesion, observed in the subsequent loading cycles, is responsible for the shape lock. When the beams are separated manually or by compressed air, the stored deformation vanishes. Magnetofriction is compared to other mechanisms to classify the new concept in the field of shape memory materials.

**Keywords:** Shape memory, magnetoactive elastomer (MAE), assembled structure, magnetic attraction forces, contact pressure, friction

## 1. INTRODUCTION

The term “Shape Memory Effect” describes the ability of a material or a structure to alter its shape between different stable states as a response to external stimuli. At least one stable state is memorized by the system.<sup>1</sup> Possible applications for the shape memory effect can be found in the field of actuators, where different stable states can be used to maintain positions without an external energy supply.<sup>2,3</sup> Furthermore, a controlled repetitive shape change has been used in the field of soft robots to achieve different modes of locomotion<sup>4</sup> and to design biomedical applications.<sup>5</sup>

The shape memory effect can be triggered by stimuli with different physical origins. Two well-known activation stimuli are a mechanical loading and a temperature variation. The shape memory of thermally activated Shape Memory Polymers (SMPs), for example, is based the phase transition between the rubbery and the glassy state.<sup>6,7</sup> After the cooling, SMPs memorize the deformation that was applied in the high temperature state. The recovery of the initial shape is activated by the application of temperatures above the glass transition temperature.<sup>8</sup> To activate the shape memory without heating the environment of SMPs, recent works propose to embed magnetic particles in the polymer and use inductive heating of Magnetic (M-)SMPs for the phase transition.<sup>9,10</sup>

---

Further author information:

S. Hermann: svenja.hermann@femto-st.fr

P. Butaud: pauline.butaud@univ-fcomte.fr

G. Chevallier: gael.chevallier@univ-fcomte.fr

L. Hirsinger: laurent.hirsinger@femto-st.fr

M. Ouisse: morvan.ouisse@femto-st.fr

In Magnetic Shape Memory Alloys (M-SMAs), a shape change can be achieved by external magnetic fields due to the reorientation of martensite.<sup>2</sup> The magnetic shape memory effect in M-SMAs is temperature dependent.<sup>11</sup> Permanently magnetized magnetically Hard MagnetoActive Elastomers (H-MAEs) can also show a shape memory effect in presence of external magnetic fields.<sup>12,13</sup> The shape change occurs when the H-MAE presents regions with different orientations of the magnetic moments that align with external magnetic fields. When the external field is switched off, the elastic forces bring the H-MAE back to its initial shape. These materials are called Magnetic Shape Memory Elastomers (M-SMEs) in the following.

The activation of the phase transitions are generally slow and a temperature hysteresis has to be considered in thermally activated shape memory materials. While the deformation capacity of M-SMA is comparatively low due to the stiffness of the material, H-MAEs need to be surrounded by a magnetic field constantly to stay in the deformed configuration.

This work presents a new concept, called magnetofriction, aiming to overcome some of the challenges of the aforementioned shape memory materials. The concept is presented in the next section, followed by the introduction of the test structure which is used in this study. The experimental tests, which have been performed to study the storage of the deformed shape on a global scale and the contact state on a local scale, are presented afterwards. Two approaches for the recovery of the initial configuration are suggested in the subsequent section. Finally, magnetofriction is compared to the aforementioned shape memory strategies in order to classify the new concept.

## 2. CONCEPT: SHAPE MEMORY BY MAGNETOFRICTION

The concept for shape memory in this work is based on the competing strength of elastic forces and magnetically induced friction forces. Friction forces occur in the contact interfaces of assembled structures. They depend on the contact pressure which maintains the assembly together.

In a MagnetoFriction - Shape Memory Polymer (MF-SMP), the contact pressure is established magnetically. An MF-SMP is assembled from permanently magnetized H-MAEs. Due to the magnetization, magnetic attraction forces develop between the H-MAEs. The magnetic forces establish the pressure in the contact interface that maintains the MF-SMP assembled (Fig. 1, “Initial, stable state”).

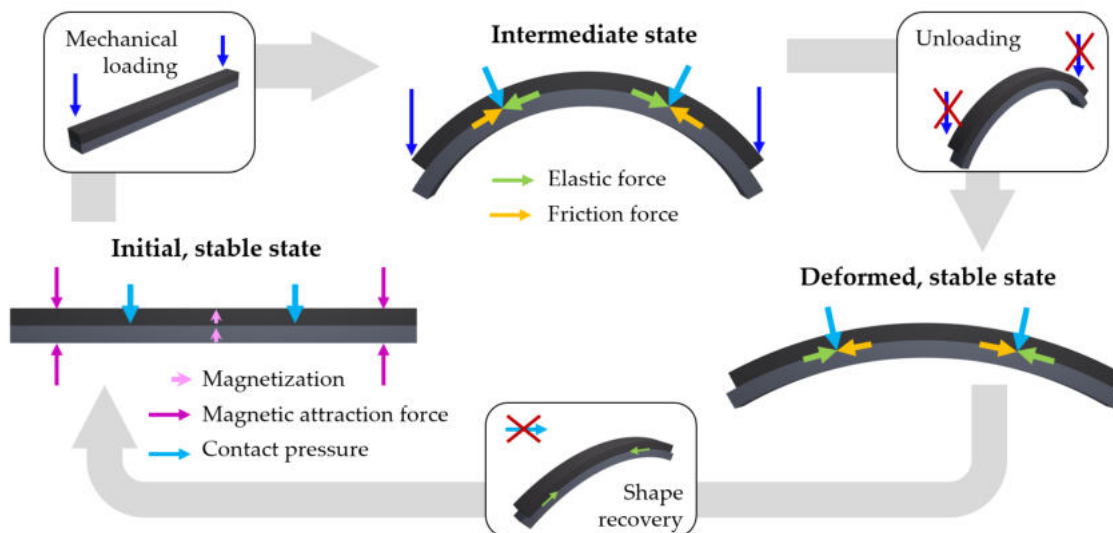


Figure 1. Illustration of the deformation cycle of a MagnetoFriction Shape Memory Polymer (MF-SMP) assembled from two magnetized magnetically hard magnetoactive elastomers.

The H-MAEs are elastic and have a low mechanical stiffness. The assembled MF-SMP can hence easily be deformed. When the assembly is deformed, elastic stresses appear in the material and generate constraints in the interface. According to Coulomb’s friction law, friction forces maintain the adhesion between two points of the contact interface up to a specific threshold that depends on the material pairing. When the elastic constraints in the H-MAEs generate forces in the interface that exceed the friction forces, the contact surfaces slide over each other. The sliding releases a part of the elastic constraints in the assembly. As the elastic constraints in the interface are decreased by the sliding, the contact state changes from sliding to adhesion. The H-MAEs stick together once again due to the magnetically induced contact pressure (Fig. 1, “Intermediate state”).

When the mechanical loading is released, the elastic forces tend to bring each H-MAE back to its initial shape. They deform the MF-SMP and also generate restoring forces in the contact interface. In the interface, however, the restoring forces have to work against the friction forces. As a result, only a part of the applied deformation is restored as long as the friction forces are present (Fig. 1, “Deformed, stable state”). When the magnetic attraction forces disappear, the friction forces vanish and the elastic forces bring the parts of the assembly back into their initial shape. The restoring of the contact pressure completes the shape memory cycle.

### 3. DESIGN OF A MAGNETOFRICTION SHAPE MEMORY POLYMER

To prove the concept of magnetofriction a test structure is assembled from two H-MAE beams. The H-MAE in this study consists of 36 vol % NdFeB particles which are randomly dispersed in a silicone matrix. The composite material has a residual flux density of approximately 0.29 T and its storage modulus lies in the order of magnitude between 1 MPa and 10 MPa. After being exposed to a strong magnetic field, the composite remains magnetized, comparable to a stiff permanent magnet.<sup>14,15</sup>

Fig. 2a illustrates the flexibility of the H-MAE as well as its response to magnetic stimuli. A MAE beam is attached on the left end and deformed by the magnetic interactions with the magnet on the upper right side of the image. The geometric dimensions of the beams in the assembly are 60 mm × 6 mm × 3 mm (length × width × thickness). Both beams are magnetized in the direction of their thickness. In the assembly, they are stacked such as their magnetization points in the same direction (Fig. 2b). The magnetic attraction forces clamp the beams together and they stick to each other without the need for glue for the assembly.

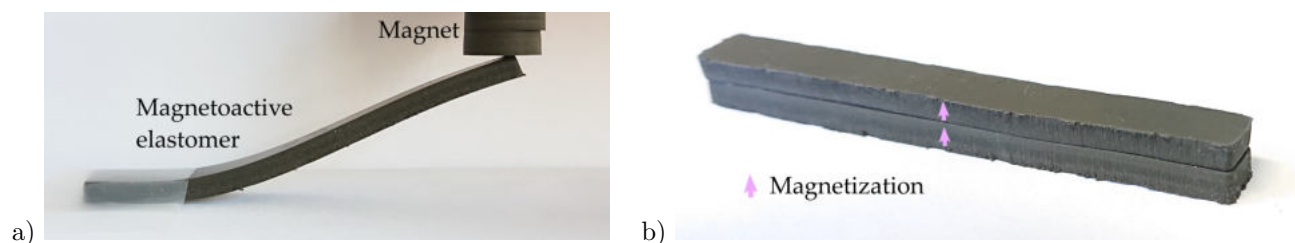


Figure 2. Single magnetized H-MAE beam, attached on the left side and deformed by magnetic interactions with a magnet (a) and the magnetofriction shape memory polymer (MF-SMP) assembled from two magnetized H-MAE beams (b).

The capacity of the assembly to stay in a deformed shape is demonstrated in a simple test illustrated in Fig. 3. The assembly is clamped in a cantilevered configuration (Fig. 3a), deformed manually (Fig. 3b) and does not deform back to its initial shape after being released (Fig. 3c). However, the material does not stay in the configuration of the maximum deformation due to the elastic restoring forces in the beams. The initial configuration can be restored by a separation of the beams (cf. Section 5). The experiments presented in the following section are performed to study the magnetofriction effect in the MF-SMP.



Figure 3. Illustration of the deformation storage in the MagnetoFriction Shape Memory Polymer (MF-SMP).

## 4. STORAGE OF A DEFORMED SHAPE

### 4.1 Experimental setup

Three-point bending tests are performed with the MF-SMP. The test rig (Fig. 4a) is composed of a mechanical measurement setup, used to apply a loading and to measure the reaction forces, and an optic measurement setup used to record images for a digital image correlation (DIC). The MF-SMP is positioned on the lower fixed part of the bending support in a dynamic mechanical analyzer (Fig. 4b). The displacement of the upper mobile part is controlled while the reaction force of the MF-SMP is measured with a unidirectional load cell, connected to the lower part (Fig. 4c). A lubricant is used to reduce the friction in the contact between the assembly and the bending test support.

The test is composed of different steps (cf. Fig. 6a). After a first loading phase, a cyclic loading is applied to evaluate if the relative position of the beams changes continuously. Five loading cycles with an amplitude of 1.5 mm are performed around an average displacement of about 2 mm. A complete unloading is prevented since the reaction force can only be measured when the assembly is in contact with the mobile part of the testing machine. The displacement velocity is set to 0.12 mm/s. After the cyclic loading, the average displacement is maintained during five minutes. This test is performed to analyze if the beam adapts to the constant loading by a sliding in the interface. In the last step, the loading is removed.

The test is filmed with a camera in order to perform the DIC later. The camera lens is arranged orthogonal to the specimen and points on the side of the assembly (Fig. 4c). An additional lighting source is used to improve the image quality. The light reflected by the metallic particles in the beam is sufficient to obtain a good contrast in the image which is important for the DIC. The images are recorded with a frequency of 2 Hz.

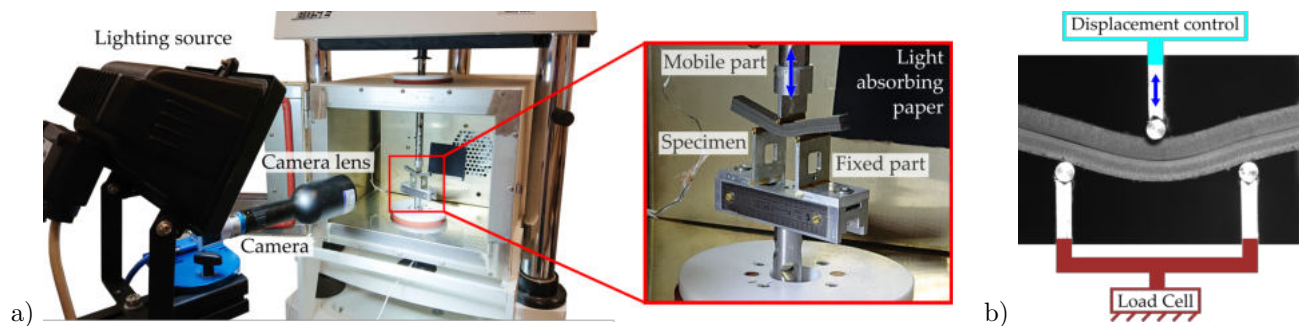


Figure 4. Experimental setup (a) and camera view of the test supplemented by schemes that illustrate the test configuration (b).

The force and displacement data are obtained as txt files from the machine and are converted from absolute to relative values during the post processing. For the digital image correlation, in-house algorithms are used to evaluate the camera images (.tiff). Boundaries and the contact interface are detected based on the contrast in the image. For the analysis of the local contact state, the position of regions of pixels has been traced by the help of a cross correlation that allows to recognize luminosity patterns.

## 4.2 Global results: deformed shape reaction force

In the first study step of the deformation storage, the initial and the final shapes of the assembly are compared. Fig. 5a and Fig. 5b show the camera images of the two cases. The images also show the contact interface detected during the post-processing. By comparing the two images, a shape change of the MF-SMP can be observed. The existence of a permanent deformation after the test is confirmed by the calculation of the displacement  $u_2$ , corresponding to the difference between the interface positions before and after the test (Fig. 5c).

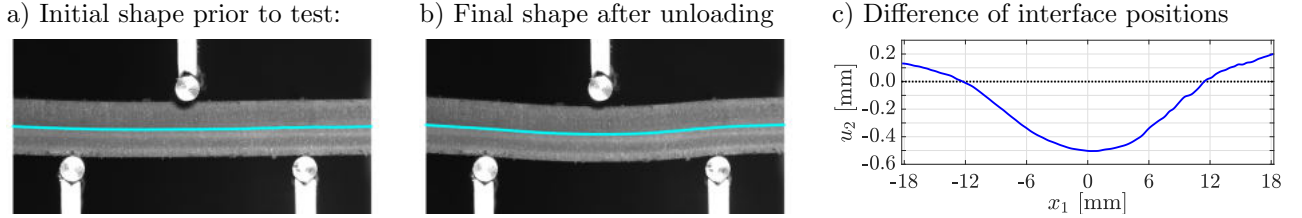


Figure 5. Camera images of the MF-SMP including the contact interface detected during the post processing (cyan) prior to the test (a) and 1 min after the mechanical loading (b) and difference between the interface positions in the two camera images  $u_2$  (c).

The response of the MF-SMP to the first loading and the subsequent five loading cycles is analyzed in the following. Fig. 6a shows the corresponding displacement of the mobile setup part during the test and Fig. 6b shows the force-displacement relation obtained for the MF-SMP. The elliptic shape of the loading cycles indicates the dissipative behavior of the assembly. The slope of the loading cycles and the beginning of the first loading path is similar. However, the sliding between the two parts which appears quite soon generates a significantly lower reaction force compared to the first loading (cf. point B in Fig. 6b).

The presence of magnetofriction can explain this behavior. During the first loading, the sticking threshold is exceeded in the contact interface and the beams start to slide over each other. A part of the constraints is released by the sliding. Due to the magnetic attraction forces, the beams stick together in a deformed shape. The force-displacement relations of the five loading cycles are similar, which indicates that the loading is applied around a new, stabilized state. The existence of a stabilized state that persists after the test can explain the permanent deformation observed in Fig. 5c. The local contact state is analyzed in the following to check this hypothesis.

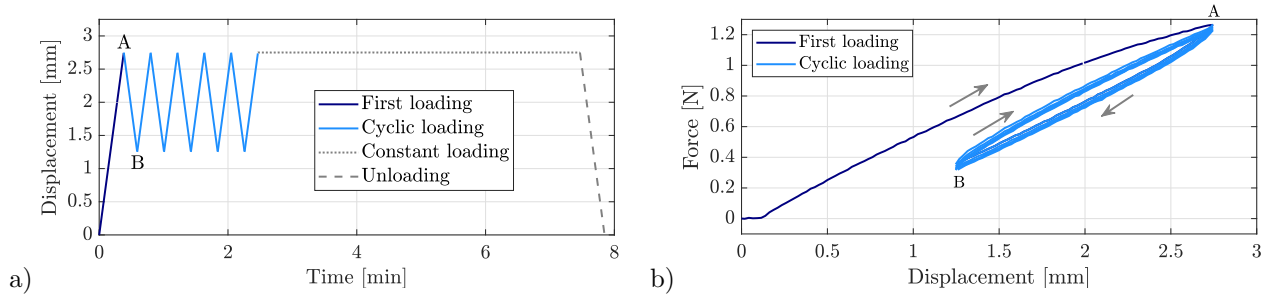


Figure 6. Displacement curve (a) highlighting the first loading and the subsequent five loading cycles blue and corresponding force-displacement relation of the MF-SMP (b).

## 4.3 Local result: contact state in the interface

The analysis of the local contact state is supposed to reveal if there is sliding in the contact interface. In the present example, a region near the interface in which both beams are visible has been chosen for the evaluation. The region is highlighted by a red contour in the camera images (upper line) and the luminosity diagrams (lower line) of Fig. 7. The luminosity gradient is used to compare the relative positions of the upper and the lower beam for different steps of the experiment.

The lower image of Fig. 7a shows the evaluation region before the test. A pixel zone has been chosen in each beam for the tracing. Prior to the loading, the pixel zone in the upper beam (zone U) is located to the left of the pixel zone in the lower beam (zone L). When the first loading reaches its maximum (Fig. 7b), the zone U is now located to the right of the zone L. The sliding, which leads to the change of the relative positions is clearly visible in the intermediate images between the two states shown in Fig. 7a and Fig. 7b.

The distance between the pixel zones becomes slightly smaller after the first unloading but the zone U remains on the right side of the zone L (Fig. 7c). This results confirms the hypothesis from the previous paragraph: the beams slide over each other during the first loading but the deformed configuration remains stable during the cyclic loading. In addition, the pixel zones maintain their relative positions even after the unloading (Fig. 7d). The relative movement of the two beams has been observed in several regions of the MF-SMP which confirms that the deformed shape is obtained by magnetofriction.

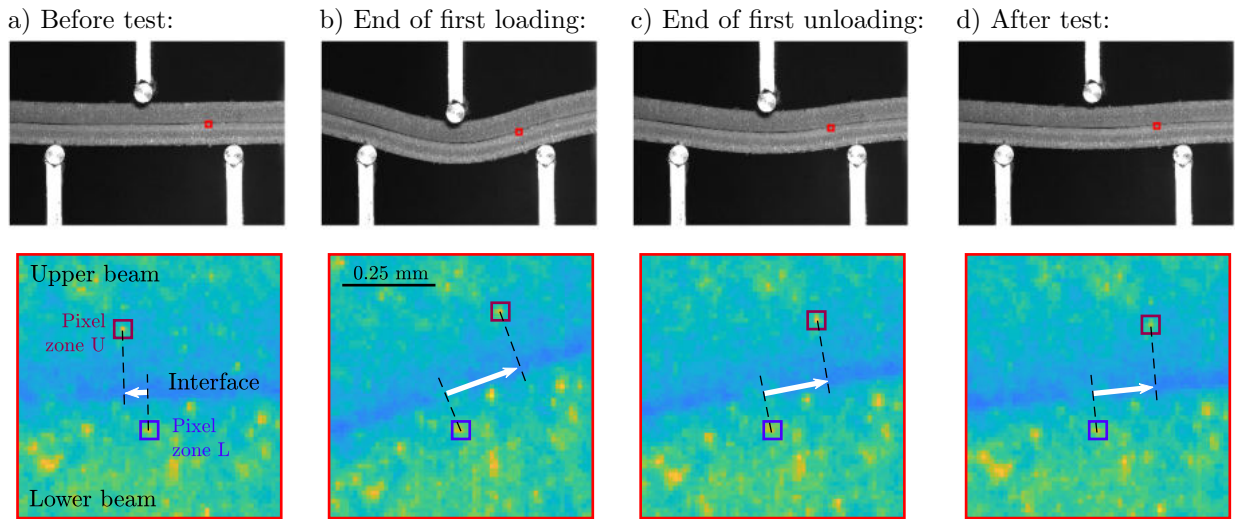


Figure 7. Camera images (upper line) and luminosity diagrams in a small region of the beam (lower line) obtained before the test (a), after the first unloading phase (b, cf. Fig. 6, point A), after the first unloading phase (c, cf. Fig. 6, point B) and one minute after the test (d).

## 5. RECOVERY OF THE INITIAL SHAPE

For the shape recovery of the MF-SMP, the contact pressure that generates the friction forces has to be suppressed. The easiest solutions for this is the separation of the two beams. The separation can be performed manually (Fig. 8a). When the beams are brought near each other after the separation, the magnetic attraction forces restore the contact. Another possibility for the shape recovery is the a separation by an air flow between the beams (Fig. 8b). A tube is inserted in the clamping of the assembled structure and the air flow is strong enough to overcome the magnetic attraction forces between the beams. Due to the magnetic attraction forces, the beams stick together once the air flow is stopped.

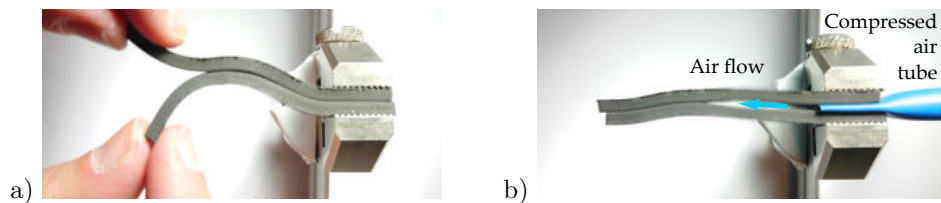


Figure 8. Recovery of the initial shape by separation of the magnetized beams in the MF-SMP: manual separation of the beams (a) and separation of the beams by an air flow in the interface (b).

While the flexibility of the beams is an advantage for the deformation storage, it is a challenge for the recovery of the exact initial shape. Due to the magnetic forces, the beams attract each other when their distance is small enough. As a result, it is difficult to adjust the beams in their exact initial configuration after a separation of the beams. The restoring of the initial shape will hence be one of the challenges for future works.

## 6. MAGNETOFRICTION COMPARED TO COMMON SHAPE MEMORY MECHANISMS

After the proof of the magnetofriction concept, the MF-SMP is now compared to common shape memory materials. As the concept is fairly new, it is a qualitative comparison that aims to position the new concept in the field of existing shape memory strategies. The comparison is detailed with reference to table 1, in which different materials have been chosen to represent a shape memory mechanism.

In the MF-SMP, the effect is instantly activated when the adhesion threshold is exceeded in the contact interface. Concerning the time constant, it is more similar to the magnetically activated M-SMA and M-SME than to thermally activated SMP. The MF-SMP is therefore well suited for applications which require fast actuation cycles.

The stiffness of the MF-SMP in its stable state lies below the stiffness of the M-SMA and the SMP. It is comparable to the stiffness of M-SME. Possible applications can therefore be found in similar fields like soft robotics or soft actuators for biomedical applications. In view of these application fields, the high shape change capacity of MF-SMP is an advantage.

In contrast to M-SME, MF-SMPs are capable to lock the shape of the deformed configuration without an external stimulus. M-SMEs remain deformed in a deformed shape only in presence of external magnetic fields. Therefore, MF-SMPs are favorable for applications in which stable states need to be maintained over a long time. While M-SMAs recover their initial shape the most precisely, the degree of shape recovery is slightly lower in the polymer materials.

The comparison of the different materials offers perspectives for future work on MF-SMP. Studies that quantify important aspects like the activation time or the stiffness variation during the transition could be performed. Additional important points for future studies are the magnetically induced contact pressure and the friction threshold in the MF-SMP

Table 1. Qualitative comparison of the properties of different shape memory alloys: Shape Memory Polymers (SMP), Magnetic Shape Memory Alloys (M-SMA), Magnetic Shape Memory Elastomers (M-SME) and the MagnetoFriction Shape Memory Polymer (MF-SMP) of this work.

| Criteria                        | SMP <sup>8,16</sup>       | M-SMA <sup>2,17</sup>   | M-SME <sup>12</sup>     | MF-SMP                  |
|---------------------------------|---------------------------|-------------------------|-------------------------|-------------------------|
| Material                        | Veriflex <sup>®</sup>     | Ni-Mn-Ga                | Silicone+NdFeB          | Silicone+NdFeB          |
| Activation type                 | Mechanics,<br>Temperature | Mechanics,<br>Magnetism | Mechanics,<br>Magnetism | Mechanics,<br>Magnetism |
| Stiffness (ambient temperature) | ●●○                       | ●●●                     | ●○○                     | ●○○ <sup>14</sup>       |
| Shape change capacity           | ●●●                       | ●○○                     | ●●○                     | ●●○                     |
| Self-sufficient deformed state  | ✓                         | ✓                       | ×                       | ✓                       |
| Recovery of initial shape       | ●●○                       | ●●●                     | ●●○                     | ●●○                     |

## 7. CONCLUSIONS

This paper illustrates a new, multi-physical concept for shape memory in assembled structures which is called magnetofriction. The concept is based on the sliding in the interface between the assembled materials and governed by the competing strength of elastic forces and magnetically induced friction forces. An assembly of two magnetized H-MAE that form a magnetofriction Shape Memory Polymer (MF-SMP) is used for the experimental



proof of concept. On a global scale, the storage of a deformed shape in bending tests is demonstrated. On a local scale, sliding in the interface is revealed by a digital image correlation. A manual separation and compressed air that temporarily flows through the interface are suggested as techniques for the recovery of the initial shape. The comparison of the new concept to common strategies for shape memory reveals possible application fields for magnetofriction and also helps to identify important aspects for future work on this topic.

## ACKNOWLEDGMENTS

This work has been funded by EIPHI Graduate School, ANR-17-EURE-0002.

## REFERENCES

- [1] Bengisu, M. and Ferrara, M., [*Materials that move: smart materials, intelligent design*], Springer (2018).
- [2] Kohl, M., Gueltig, M., Pinneker, V., Yin, R., Wendler, F., and Krevet, B., “Magnetic shape memory microactuators,” *Micromachines* **5**(4), 1135–1160 (2014).
- [3] Motzki, P., Khelfa, F., Zimmer, L., Schmidt, M., and Seelecke, S., “Design and validation of a reconfigurable robotic end-effector based on shape memory alloys,” *IEEE/ASME Transactions on Mechatronics* **24**(1), 293–303 (2019).
- [4] Hu, W., Lum, G. Z., Mastrangeli, M., and Sitti, M., “Small-scale soft-bodied robot with multimodal locomotion,” *Nature* **554**, 81–85 (2018).
- [5] Buckley, P., McKinley, G.H. and Wilson, T., Small, W., Bennett, W., Bearinger, J., McElfresh, M., and Maitland, D., “Inductively heated shape memory polymer for the magnetic actuation of medical devices,” *IEEE Trans. Biomed. Eng.* **53**, 2075–2083 (2006).
- [6] Diani, J., Gilormini, P., Frédy, C., and Rousseau, I., “Predicting thermal shape memory of crosslinked polymer networks from linear viscoelasticity,” *Int. J. Solids Struct.* **49**(5), 793–799 (2012).
- [7] Butaud, P., Renault, D., Verdin, B., Ouisse, M., and Chevallier, G., “In-core heat distribution control for adaptive damping and stiffness tuning of composite structures,” *Smart Materials and Structures* **29**(6), 065002 (2020).
- [8] Butaud, P., Placet, V., Klesa, J., Ouisse, M., Foltête, E., and Gabrion, X., “Investigations on the frequency and temperature effects on mechanical properties of a shape memory polymer (veriflex),” *Mech. Mater.* **87**, 50–60 (2015).
- [9] Schmidt, A. M., “Electromagnetic activation of shape memory polymer networks containing magnetic nanoparticles,” *Macromolecular Rapid Communications* **27**(14), 1168–1172 (2006).
- [10] Ze, Q., Kuang, X., Wu, S., Wong, J., Montgomery, S., Zhang, R., Kovitz, J., Yang, F., Qi, H., and Zhao, R., “Magnetic shape memory polymers with integrated multifunctional shape manipulation,” *Advanced Materials* **32**(4), 1906657 (2020).
- [11] Kiefer, B. and Lagoudas, D., “Magnetic field-induced martensitic variant reorientation in magnetic shape memory alloys,” *Philosophical Magazine*, 4289–4329 (2005).
- [12] Kim, Y., Yuk, H., Zhao, R., Chester, S., and Zhao, X., “Printing ferromagnetic domains for untethered fast-transforming soft materials,” *Nature* **558**, 274–291 (2018).
- [13] Qi, S., Guo, H., Fu, J., Xie, Y., Zhu, M., and Yu, M., “3d printed shape-programmable magneto-active soft matter for biomimetic applications,” *Composites Science and Technology* **188**, 107973 (2020).
- [14] Hermann, S., Butaud, P., Chevallier, G., Manceau, J.-F., and Espanet, C., “Magnetic and dynamic mechanical properties of a highly coercive mre based on ndfeb particles and a stiff matrix,” *Smart Mater. Struct* **29**, 105009 (2020).
- [15] Hermann, S., Espanet, C., Butaud, P., Chevallier, G., Manceau, J.-F., and Hirsinger, L., “Modelization of the coupled behavior of a magnetically hard magnetoactive elastomer,” in [*Constitutive Models for Rubber XI*], 122–127, CRC Press (2019).
- [16] Ivens, J., Urbanus, M., and De Smet, C., “Shape recovery in a thermoset shape memory polymer and its fabric-reinforced composites,” *Express Polymer Letters* **5**(3), 254–261 (2011).
- [17] Segui, C., Cesari, E., Pons, J., and Chernenko, V., “Internal friction behavior of Ni-Mn-Ga,” *Materials Science and Engineering: A* **73**(1–2), 481–484 (2004).